

## Silicon Doping in Ba<sub>2</sub>In<sub>2</sub>O<sub>5</sub>: Example of a Beneficial Effect of Silicon Incorporation on Oxide Ion/Proton Conductivity

J. F. Shin,<sup>†</sup> D. C. Apperley,<sup>‡</sup> and P. R. Slater<sup>\*,†</sup>

<sup>†</sup>School of Chemistry, University of Birmingham, Birmingham. B15 2TT. U.K., and

<sup>‡</sup>Department of Chemistry, Durham University, South Road, Durham. DH1 3LE. U.K.

Received July 26, 2010. Revised Manuscript Received September 18, 2010

In the solid oxide fuel cell (SOFC) field, the presence of silicon impurities is commonly considered to be detrimental to the performance due to segregation as silica at the grain boundaries. In this paper we demonstrate, however, that silicon doping into Ba<sub>2</sub>In<sub>2</sub>O<sub>5</sub> leads to a significant enhancement in the oxide ion conductivity. The results indicate that silicon is incorporated into the structure leading to a conversion from an ordered brownmillerite-type structure to a disordered perovskite-type, with the oxygen vacancy disordering leading to the conductivity enhancement. In wet atmospheres, the conductivity is further enhanced through a protonic contribution, leading to conductivities ( $2.4 \times 10^{-3} \text{ Scm}^{-1}$  at 400 °C) comparable to the best perovskite proton conductors. Thus, the results show that silicon can be incorporated into the perovskite structure, suggesting further studies in this area are warranted, particularly related to electrode materials.

### Introduction

Materials displaying high oxide ion conductivity have attracted considerable attention due to potential applications in solid oxide fuel cells, oxygen sensors, and separation membranes. A wide number of structure types have been investigated for such applications, with the vast majority of research focusing on materials with the fluorite or perovskite structure.<sup>1,2</sup> There has been a considerable amount of work aimed at the optimization of such oxide ion conductors, and the presence of silicon containing impurities has been reported to be detrimental to the performance, particularly for fluorite based systems, where it has been reported that the silicon collects as silica at the grain boundaries.<sup>3–5</sup> As a result, it is generally considered that silicon is a poison for fuel cell materials and great care should be taken to eliminate possible contamination with it. Recently we have been investigating the possibility of doping tetrahedral oxyanions into perovskite systems of relevance to fuel cell materials. In our initial work we investigated phosphate doping into Ba<sub>2</sub>In<sub>2</sub>O<sub>5</sub>,<sup>6</sup> which contains ordered oxide ion vacancies such that the room-temperature structure contains alternating layers of InO<sub>6</sub> octahedra and InO<sub>4</sub> tetrahedra. This vacancy ordering leads to rather low oxide ion conductivity at low temperatures, with the observation of a discontinuous jump in oxide ion conductivity by more than

an order of magnitude at a temperature of  $\approx 930$  °C. This can be explained by a phase change from orthorhombic to tetragonal resulting in disordering of these oxygen vacancies.<sup>7,8</sup> Our recent work demonstrated the successful incorporation of the phosphate anion into Ba<sub>2</sub>In<sub>2</sub>O<sub>5</sub>, leading to stabilization of the cubic cell along with enhanced conductivity,<sup>6</sup> similar to traditional doping strategies on the In site with higher valent cations of similar size (e.g., Sn, Ti, V, Mo, and W).<sup>9–12</sup> In this paper, we extend this work to examine whether stabilization of the cubic phase can be achieved by doping with silicon, where incorporation would be expected as the tetrahedral anion, SiO<sub>4</sub><sup>4-</sup>. The results demonstrate this to be the case, leading to a significant enhancement in performance.

### Experimental Section

High-purity BaCO<sub>3</sub>, In<sub>2</sub>O<sub>3</sub>, and SiO<sub>2</sub> were used to prepare Ba<sub>2</sub>In<sub>2–x</sub>Si<sub>x</sub>O<sub>5+x/2</sub> ( $x = 0, 0.1, 0.2, 0.3$ ) samples. To overcome Ba loss at elevated temperatures, a 3% excess of BaCO<sub>3</sub> was employed. Without this small Ba excess, low levels of Ba deficient impurity phases, such as BaIn<sub>2</sub>O<sub>4</sub> and Ba<sub>4</sub>In<sub>6</sub>O<sub>13</sub>, were observed after sintering, as has been seen in other studies synthesizing similar Ba-containing phases.<sup>13,14</sup> The powders were intimately ground

\*Corresponding author address: School of Chemistry, University of Birmingham, Birmingham B15 2TT UK; e-mail: p.r.slater@bham.ac.uk.

- (1) Goodenough, J. B. *Annu. Rev. Mater. Res.* **2003**, *33*, 91.
- (2) Orera, A.; Slater, P. R. *Chem. Mater.* **2010**, *22*, 675.
- (3) Aoki, M.; Chiang, Y. M.; Kosacki, I.; Lee, I. J. R.; Tuller, H.; Liu, Y. P. *J. Am. Ceram. Soc.* **1996**, *79*, 1169.
- (4) Badwal, S. P. S.; Ciacchi, F. T.; Rajendran, S.; Drennan, J. *Solid State Ionics* **1998**, *109*, 167.
- (5) Appel, C. C.; Bonanos, N. *J. Euro. Ceram. Soc.* **1999**, *19*, 847.
- (6) Shin, J. F.; Hussey, L.; Orera, A.; Slater, P. R. *Chem. Commun.* **2010**, *46*, 4613.

- (7) Goodenough, J. B.; Ruizdiaz, J. E.; Zhen, Y. S. *Solid State Ionics* **1990**, *44*, 21.
- (8) Speakman, S. A.; Richardson, J. W.; Mitchell, B. J.; Misture, S. T. *Solid State Ionics* **2002**, *149*, 247.
- (9) Ta, T. Q.; Tsuji, T.; Yamamura, Y. J. *Alloys Compd.* **2006**, *408*, 253.
- (10) Schober, T. *Solid State Ionics* **1998**, *109*, 1.
- (11) Jayaraman, V.; Magrez, A.; Caldes, M.; Joubert, O.; Ganne, M.; Piffard, Y.; Brohan, L. *Solid State Ionics* **2004**, *170*, 17.
- (12) Rolle, A.; Vannier, R. N.; Giridharan, N. V.; Abraham, F. *Solid State Ionics* **2005**, *176*, 2095.
- (13) Omata, T.; Fuke, T.; Otsuka-Yao-Matsuo, S. *Solid State Ionics* **2006**, *177*, 2447.
- (14) Abakumov, A. M.; Rossell, M. D.; Gutnikova, O. Y.; Drozhzhin, O. A.; Leonova, L. S.; Dobrovolsky, Y. A.; Istomin, S. Y.; Van Tendeloo, G.; Antipov, E. V. *Chem. Mater.* **2008**, *20*, 4457.

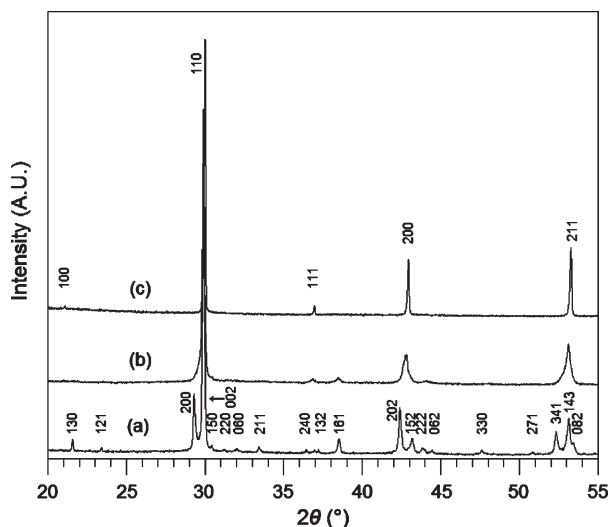


**Figure 1.** X-ray diffraction patterns for  $\text{Ba}_2\text{In}_{2-x}\text{Si}_x\text{O}_{5+x/2}$ :  $x$  = (a) 0, (b) 0.1, and (c) 0.2.

and heated initially to 1000 °C for 12 h, before ball-milling (350 rpm for 1 h, Fritsch Pulverisette 7 Planetary Mill) and reheating to 1000 °C for a further 50 h. The resulting powders were then pressed as pellets (1.3 cm diameter) and sintered at 1400 °C for 10 h. To limit the amount of Ba loss during the sintering process, the pellets were covered in sample powder and the crucible was covered with a lid. Phase purity was determined using X-ray powder diffraction (Bruker D8 diffractometer with  $\text{Cu K}\alpha_1$  radiation). To provide information regarding the silicate environment, Raman spectroscopy measurements were made using a Renishaw inVia Raman microscope with excitation using a Cobolt Samba CW 532 nm DPSS Laser. In addition,  $^{29}\text{Si}$  NMR data were also collected, obtained using a Varian Unity Inova operating at 59.56 MHz for  $^{29}\text{Si}$ . Spectral referencing was with respect to tetramethylsilane.

For the conductivity measurements, the sintered pellets (>87% theoretical density) were coated with Pt paste, and then heated to 750 °C for 1 h to ensure bonding to the pellet. Conductivities were then measured by AC impedance measurements (Hewlett-Packard 4182A impedance analyzer) in the range from 0.1 to  $10^3$  kHz. Because  $\text{Ba}_2\text{In}_2\text{O}_5$  displays a small but significant p-type contribution to the conductivity in oxidizing conditions, measurements were made in dry  $\text{N}_2$  to eliminate this contribution. In addition measurements were made in wet  $\text{N}_2$  (in which the gas was bubbled at room temperature through water) to identify any protonic contribution to the conductivity. The impedance data showed a single broad semicircle in both dry and wet atmospheres. The capacitance of the semicircle was typical of a bulk response, suggesting that the resistance of the grain boundary was small compared to that of the bulk.

## Results and Discussion

X-ray powder diffraction analysis showed that on Si doping there was a change in symmetry from orthorhombic for  $\text{Ba}_2\text{In}_2\text{O}_5$  to cubic for  $\text{Ba}_2\text{In}_{1.8}\text{Si}_{0.2}\text{O}_{5.1}$  (Figure 1). For higher Si levels, small  $\text{Ba}_2\text{SiO}_4$  impurities were observed indicating a solubility limit of  $\approx 10\%$ . Calculated cell parameters are given in Table 1, with the variation in cubic equivalent cell volume shown in Figure 2. The latter shows a decrease in volume with increasing Si content due to the smaller size of  $\text{Si}^{4+}$  versus  $\text{In}^{3+}$  having a greater

**Table 1.** Cell Parameter Data for  $\text{Ba}_2\text{In}_{2-x}\text{Si}_x\text{O}_{5+x/2}$

| sample<br>(nominal composition)                            | unit cell parameters (Å) |           |          | unit cell<br>volume (Å <sup>3</sup> ) |
|--|--------------------------|-----------|----------|---------------------------------------|
|  | <i>a</i>                 | <i>b</i>  | <i>c</i> |                                       |
| $\text{Ba}_2\text{In}_2\text{O}_5$                         | 6.089(2)                 | 16.736(8) | 5.963(2) | 607.6(2)                              |
| $\text{Ba}_2\text{In}_{1.9}\text{Si}_{0.1}\text{O}_{5.05}$ | 6.012(5)                 | 16.794(5) | 5.962(6) | 602.0(4)                              |
| $\text{Ba}_2\text{In}_{1.8}\text{Si}_{0.2}\text{O}_{5.1}$  | 4.209(1)                 |           |          | 74.6(1)                               |

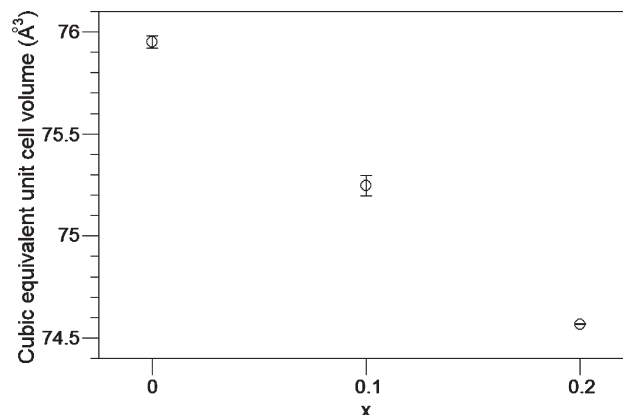


**Figure 2.** Variation of cubic equivalent unit cell volume with silicate content for  $\text{Ba}_2\text{In}_{2-x}\text{Si}_x\text{O}_{5+x/2}$ .

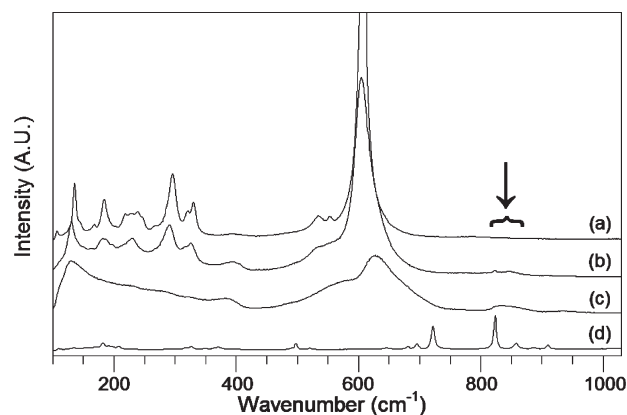
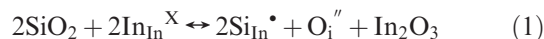


**Figure 3.** Raman spectra of  $\text{Ba}_2\text{In}_{2-x}\text{Si}_x\text{O}_{5+x/2}$ ,  $x$  = (a) 0, (b) 0.1, and (c) 0.2, showing the emergence of bands due to the presence of silicate (most intense bands highlighted). For comparison, the Raman spectrum for (d)  $\text{Ba}_2\text{SiO}_4$  is included.

influence than the effect of increasing the oxygen content. The extra oxygen incorporated as a result of the higher charge on  $\text{Si}^{4+}$  versus  $\text{In}^{3+}$  can be accommodated within the vacant interstitial sites in the tetrahedral layer of the brownmillerite structure: in terms of a defect equation, we can write the following



This increase in oxygen content would be expected to disrupt the oxygen vacancy ordering in the parent brownmillerite structure, with the resulting oxygen disorder accounting for the increase in cell symmetry observed by X-ray diffraction.

The Raman spectroscopy data are shown in Figure 3. These data show a reduction in the intensity of the In–O peaks, most clearly seen in the peaks around 600  $\text{cm}^{-1}$ ,

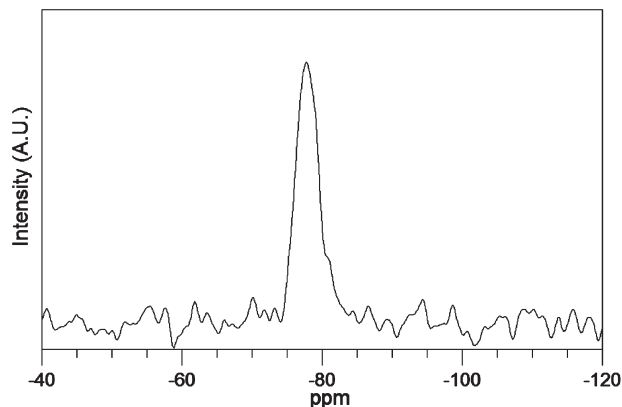


Figure 4.  $^{29}\text{Si}$  NMR spectrum for  $\text{Ba}_2\text{In}_{1.8}\text{Si}_{0.2}\text{O}_{5.1}$ .

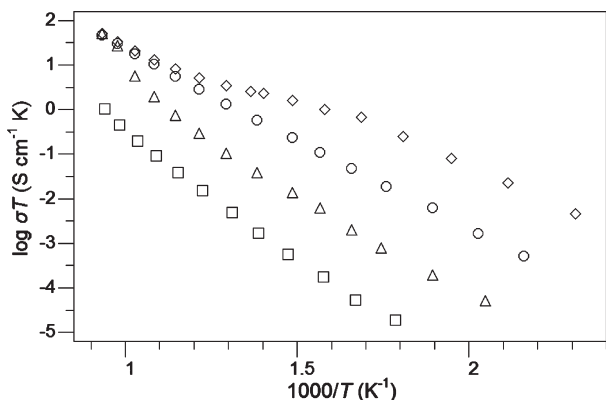


Figure 5. Conductivity data in dry  $\text{N}_2$  for  $\text{Ba}_2\text{In}_{2-x}\text{Si}_x\text{O}_{5+x/2}$  where  $x = 0$  (open square),  $x = 0.1$  (open triangle),  $x = 0.2$  (open circle); and wet  $\text{N}_2$  for  $x = 0.2$  (open diamond).

along with the emergence of peaks due to silicate. The latter are in the region  $800\text{--}900\text{ cm}^{-1}$ , similar to that observed for  $\text{Ba}_2\text{SiO}_4$ , and consistent with the Si being tetrahedrally coordinated. Here it should be noted that for a perfectly cubic perovskite (space group  $Pm3m$ ), there should be no Raman active bands, with the exception of possible second-order effects.<sup>15,16</sup> The observation of Raman active bands would therefore suggest that although the average structure is cubic, as shown by X-ray diffraction, there is some local deviation from cubic symmetry.

The  $^{29}\text{Si}$  NMR spectrum for  $\text{Ba}_2\text{In}_{1.8}\text{Si}_{0.2}\text{O}_{5.1}$  (Figure 4) shows a single peak at a chemical shift of  $-77.8\text{ ppm}$ , which is consistent with tetrahedral Si ( $\text{Q}^0$ ), in agreement with the Raman data. The observed chemical shift is more negative than that reported for  $\text{Ba}_2\text{SiO}_4$  ( $-70.3\text{ ppm}$ ),<sup>17</sup> which can be correlated with the fact that there are interactions with both Ba and In in the present samples.

Previous reports on the effect of silicon on SOFC electrolytes such as yttria stabilized zirconia had indicated a detrimental effect on the conductivity, attributed to its segregation as silica at the grain boundaries.<sup>3–5</sup> Therefore it was important to address the effect on the conductivity in this

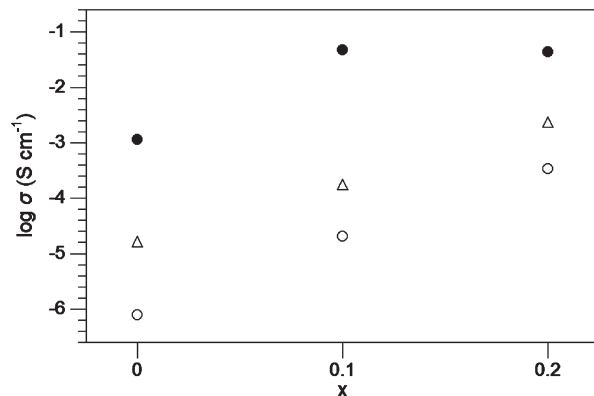


Figure 6. Variation in  $\sigma_{800\text{C}}$  (filled circles) and  $\sigma_{400\text{C}}$  (open circles) in dry  $\text{N}_2$  for  $\text{Ba}_2\text{In}_{2-x}\text{Si}_x\text{O}_{5+x/2}$ . Data for  $\sigma_{400\text{C}}$  in wet  $\text{N}_2$  included as open triangles.

Table 2. Conductivity Data for  $\text{Ba}_2\text{In}_{2-x}\text{Si}_x\text{O}_{5+x/2}$  (At Higher Temperatures ( $> 650^\circ\text{C}$ ), the Conductivities in Dry and Wet Conditions Are the Same)

| sample (nominal composition)                               | conductivity ( $\text{S cm}^{-1}$ ) |                      |                      |
|--|-------------------------------------|----------------------|----------------------|
|  | 400 $^\circ\text{C}$                |                      | 800 $^\circ\text{C}$ |
|  | wet                                 | dry                  |                      |
| $\text{Ba}_2\text{In}_2\text{O}_5$                         | $1.6 \times 10^{-5}$                | $7.6 \times 10^{-7}$ | $1.2 \times 10^{-3}$ |
| $\text{Ba}_2\text{In}_{1.9}\text{Si}_{0.1}\text{O}_{5.05}$ | $1.8 \times 10^{-4}$                | $2.0 \times 10^{-5}$ | $4.7 \times 10^{-2}$ |
| $\text{Ba}_2\text{In}_{1.8}\text{Si}_{0.2}\text{O}_{5.1}$  | $2.4 \times 10^{-3}$                | $3.4 \times 10^{-4}$ | $4.3 \times 10^{-2}$ |

case. These data showed that on Si doping there was a significant enhancement in the low temperature conductivity (Figures 5 and 6). The data showed that at low temperatures, the conductivity increased substantially with increasing Si content. Thus at  $400^\circ\text{C}$  in dry  $\text{N}_2$ , the introduction of 10% Si leads to an increase in conductivity by nearly 3 orders of magnitude (Table 2). The increase in conductivity can be correlated with the Si doping leading to increasing disorder on the oxygen sublattice, as evidenced by the change in cell symmetry to cubic for 10% Si doping. At higher temperatures ( $800^\circ\text{C}$ ), the conductivities of the 5% and 10% Si doped samples were similar, with some indication for a small decrease for the 10% Si doped sample. This can be explained by the fact that at these elevated temperatures, both these samples now have significant disorder on the oxygen sublattice. The small decrease in conductivity for the 10% Si doped samples could be related to the reduction in available vacant anion sites in the structure, as a result of the increase in oxygen content on Si doping, or it could indicate a small degree of defect trapping: a similar effect was observed previously on phosphate doping.<sup>6</sup>

A further enhancement in the conductivity was observed by changing the atmosphere to wet  $\text{N}_2$ , which can be accounted for by water incorporation, according to the defect eq 2, similar to that previously reported for undoped  $\text{Ba}_2\text{In}_2\text{O}_5$ .<sup>18,19</sup>



As is typical in proton conducting ceramics,<sup>19,20</sup> the water and hence proton incorporation is most significant at lower temperatures. Thus, at temperatures below  $\approx 350^\circ\text{C}$ , all

(15) Karlsson, M.; Matic, A.; Knee, C. S.; Ahmed, I.; Eriksson, S. G.; Borjesson, L. *Chem. Mater.* **2008**, *20*, 3480.

(16) Karlsson, M.; Ahmed, I.; Matic, A.; Eriksson, S. G. *Solid State Ionics* **2008**, *181*, 126.

(17) Magi, M.; Lippmaa, E.; Samoson, A.; Engelhardt, G.; Grimmer, A.-R. *J. Phys. Chem.* **1984**, *88*, 1518.

(18) Fisher, C. A. J.; Islam, M. S. *Solid State Ionics* **1999**, *118*, 355.

(19) Norby, T.; Larring, Y. *Curr. Opin. Solid State Mater. Sci.* **1997**, *2*, 593.

(20) Kreuer, K. D. *Annu. Rev. Mater. Res.* **2003**, *33*, 333.

samples show an order of magnitude increase in wet N<sub>2</sub>, indicative of significant proton conductivity. As the temperature increases further, the level of water incorporation decreases, and the difference between the conductivities in dry and wet atmospheres decreases, such that above  $\approx 650$  °C, the protonic contribution becomes insignificant (Figure 5). The conductivity of  $2.4 \times 10^{-3} \text{ Scm}^{-1}$  at 400 °C in wet N<sub>2</sub> for the 10% Si doped sample, Ba<sub>2</sub>In<sub>1.8</sub>Si<sub>0.2</sub>O<sub>5.1</sub>, is comparable to that of the best proton conducting perovskites, Ba(Zr/Ce)<sub>1-x</sub>Y<sub>x</sub>O<sub>3-x/2</sub>,<sup>20</sup> highlighting the strong beneficial effect of Si doping in Ba<sub>2</sub>In<sub>2</sub>O<sub>5</sub>.

### Conclusions

Contrary to the reported detrimental effect of silicon on the conductivity of fluorite based oxide ion conductors, the

results here highlight the strongly beneficial effect of silicon doping in Ba<sub>2</sub>In<sub>2</sub>O<sub>5</sub>. In light of these results, further studies of the influence of silicon in perovskite-based SOFC materials are warranted.

**Acknowledgment.** We express thanks to the University of Birmingham for funding (EPS international studentship for J.F.S.). We would also like to thank the EPSRC solid-state NMR service for data collection. The Bruker D8 diffractometer and Renishaw inVia Raman microscope used in this research were obtained through the Science City Advanced Materials project: Creating and Characterising Next generation Advanced Materials project, with support from Advantage West Midlands (AWM) and part funded by the European Regional Development Fund (ERDF).